Letter

# Floquet geometric squeezing in fast-rotating condensates

Li Chen,[1,*] Fei Zhu,[1] Yunbo Zhang,[2] and Han Pu[3]

[1]*Institute of Theoretical Physics, State Key Laboratory of Quantum Optics and Quantum Optics Devices, Shanxi University, Taiyuan 030006, China*

[2]*Zhejiang Key Laboratory of Quantum State Control and Optical Field Manipulation, and Department of Physics, Zhejiang Sci-Tech University, Hangzhou 310018, China*

[3]*Department of Physics and Astronomy, and Smalley-Curl Institute, Rice University, Houston, Texas 77005, USA*

(Received 17 July 2024; accepted 2 January 2025; published 14 January 2025)

Constructing and manipulating quantum states in fast-rotating Bose-Einstein condensates (BECs) has long stood as a significant challenge as the rotating speed approached a critical velocity. Although a recent experiment [R. J. Fletcher *et al.*, Science **372**, 1318 (2021)] has realized the geometrically squeezed state of the guiding-center mode, the remaining degree of freedom, the cyclotron mode, remains unsqueezed due to the large energy gap of the Landau levels. To overcome this limitation, in this Letter, we propose a Floquet-based state-preparation protocol by periodically driving an anisotropic potential. This protocol not only facilitates single-cyclotron-mode squeezing, but also enables two-mode squeezing. Such two-mode squeezing offers a richer set of dynamics compared to single-mode squeezing and can achieve a wave-packet width well below the lowest-Landau-level limit. Our work provides a highly controllable knob for realizing diverse geometrically squeezed states in ultracold quantum gases within the quantum Hall regime.

DOI: 10.1103/PhysRevA.111.L011303

*Introduction*. The quantum simulation of Landau levels using cold atoms holds significance for exploring topological states and discovering novel quantum phases of matter that have no counterpart in electronic materials [1–5]. Rotating Bose-Einstein condensates (BECs) provide a viable pathway for such simulations as they can mimic the motion of electrons in a gauge field [6–20]. The corresponding dynamics encompasses two degrees of freedom—the *cyclotron* mode and the *guiding-center* mode. Particularly, when the BEC is in the quantum Hall regime, i.e., the rotating frequency $\Omega$ approaching the external trapping frequency $\omega$, the effective energy of the guiding-center mode vanishes, leading to extensive level degeneracy. This degeneracy, combined with the nondegenerate cyclotron mode, gives rise to the characteristic Landau levels typically observed in charged particles in two dimensions (2D) subjected to a strong magnetic field [21,22].

Despite various advantages of rotating BECs, the precise manipulation of quantum states within the quantum Hall regime is hindered by instabilities [6,17]. In this case, the centrifugal force exactly counterbalances the confining harmonic potential, rendering the atoms in a flat-land scenario (i.e., the Landau levels) to lack effective confinement. Recently, an experiment on geometric squeezing provides an effective approach for the quantum control of BECs within the quantum Hall regime [11]. The experiment employed a quasi-2D harmonic potential with weak anisotropy, which effectively provided a transverse Hall drift [23–25]. Under its influence, the quantum fluctuation in the guiding-center phase space was suppressed, akin to degenerate parametric oscillation in quantum optics [26–29], leading to a single-mode (i.e., the guiding-center mode) squeezed state. The real-space density distribution of the BEC becomes an anisotropy Gaussian with a minimal width $\sigma_{\mathrm{LLL}}$ [11], the characteristic length of the lowest Landau level. The width $\sigma_{\mathrm{LLL}}$ arises from the unsqueezed cyclotron mode, with the associated wave function remaining in the ground state of a harmonic oscillator.

In fact, similar to the guiding-center mode, the Hamiltonian realized in the experiment also provides the necessary terms for squeezing the cyclotron mode [11]. However, due to the dominant energy gap of the Landau levels, an effective geometric squeezing of the cyclotron mode is unattainable. In other words, to achieve significant squeezing in the cyclotron mode, we need to find a way to overcome this energy gap. Motivated by this question, in this Letter, we propose a Floquet-based state-preparation protocol, in which the anisotropy of the trap is periodically modulated. We find that, when the modulation frequency $\nu$ coincides with twice the energy gap of Landau levels, the Floquet effective Hamiltonian can circumvent the aforementioned limitation and efficiently generate the squeezing of the cyclotron mode. More importantly, a protocol comprising both direct (dc) and alternating (ac) components allows for the simultaneous squeezing of both the cyclotron and the guiding-center modes, resulting in a two-mode geometrically squeezed state. In real space, the wave-packet width of the two-mode squeezed state decays exponentially and can surpass the limitation of $\sigma_{\mathrm{LLL}}$.

*Hamiltonian*. We consider the experimental setup [11]: a quasi-2D BEC being loaded into a magnetic harmonic trap.

*Contact author: lchen@sxu.edu.cn

 

The trap is rotating along the $z$ direction in angular frequency $\Omega$. In the rotating reference, the system is described by the single-particle Hamiltonian (setting $\hbar = 1$)

$$h_0 = \frac{\mathbf{p}^2}{2m} + V_{\text{ext}}(\mathbf{r}) - \Omega L_z, \tag{1}$$

where $\mathbf{r} = (x, y)$ and $\mathbf{p} = (p_x, p_y)$, $m$ is the atomic mass, $L_z = xp_y - yp_x$ the axial angular momentum operator, and $\Omega$ the rotation frequency. The external potential $V_{\text{ext}}$ is given by

$$V_{\text{ext}}(\mathbf{r}) = \frac{m(1+\varepsilon)\omega^2}{2}x^2 + \frac{m(1-\varepsilon)\omega^2}{2}y^2, \tag{2}$$

with $\varepsilon \ll 1$ being a small dimensionless parameter characterizing the anisotropy of the trap. Notably, when $\varepsilon \neq 0$, the axial rotational symmetry is broken.

To separate the cyclotron and the guiding-center modes, we perform a unitary transformation $G = \exp(-i\kappa m\omega xy)$ with $\kappa \equiv \varepsilon\omega/2\Omega$. The transformed Hamiltonian reads

$$\tilde{h}_0 = Gh_0G^\dagger = s\left[\frac{\tilde{p}^2}{2m} + \frac{m\omega^2}{2}(\tilde{x}^2 + \tilde{y}^2)\right] + \kappa\omega(\tilde{x}\tilde{p}_y + \tilde{y}\tilde{p}_x) - \Omega(\tilde{x}\tilde{p}_y - \tilde{y}\tilde{p}_x), \tag{3}$$

where $s \equiv \sqrt{1+\kappa^2}$ and

$$\tilde{\mathbf{r}} = (\tilde{x}, \tilde{y}) = s^{1/2}\mathbf{r}, \quad \tilde{\mathbf{p}} = (\tilde{p}_x, \tilde{p}_y) = s^{-1/2}\mathbf{p}. \tag{4}$$

Then, one can define two sets of independent bosonic modes: the *cyclotron mode* characterized by the ladder operator $\tilde{a}$ and quadratures $(\tilde{\xi}, \tilde{\eta})$, and the *guiding-center* mode characterized by the operator $\tilde{b}$ and quadratures $(\tilde{X}, \tilde{Y})$. The specific definitions of the mode operators are given by

$$\tilde{a} = \frac{\tilde{\xi} + i\tilde{\eta}}{\sqrt{2}l_B}, \quad \tilde{\xi} = \frac{\tilde{x}}{2} - \frac{\tilde{p}_y}{2m\omega}, \quad \tilde{\eta} = \frac{\tilde{y}}{2} + \frac{\tilde{p}_x}{2m\omega},$$

$$\tilde{b} = \frac{\tilde{X} - i\tilde{Y}}{\sqrt{2}l_B}, \quad \tilde{X} = \frac{\tilde{x}}{2} + \frac{\tilde{p}_y}{2m\omega}, \quad \tilde{Y} = \frac{\tilde{y}}{2} - \frac{\tilde{p}_x}{2m\omega}, \tag{5}$$

with $l_B \equiv 1/\sqrt{2m\omega}$ being the magnetic length of the Landau levels (see below). Notably, operators belonging to each of the two modes satisfy bosonic commutation relations, i.e.,

$$[\tilde{a}, \tilde{a}^\dagger] = [\tilde{b}, \tilde{b}^\dagger] = 1, \quad [\tilde{\xi}, \tilde{\eta}] = -[\tilde{X}, \tilde{Y}] = il_B^2, \tag{6}$$

whereas operators between the two modes mutually commute. In terms of these operators, the Hamiltonian $\tilde{h}_0$ takes a simple form of

$$\tilde{h}_0 = \tilde{\omega}_+\tilde{a}^\dagger\tilde{a} + \tilde{\omega}_-\tilde{b}^\dagger\tilde{b} - \frac{\zeta}{2}(\tilde{a}^2 - \tilde{b}^2 + \text{H.c.}), \tag{7}$$

where $\tilde{\omega}_\pm \equiv s\omega \pm \Omega$ and $\zeta \equiv \kappa\omega = \varepsilon\omega^2/2\Omega$. The separation of the cyclotron and the guiding-center modes becomes manifest. Now, $|n_{\tilde{a}}, n_{\tilde{b}}\rangle$ provides a complete set of basis, where the non-negative integers $n_{\tilde{a}}$ and $n_{\tilde{b}}$ are the quantum numbers associated with $\tilde{a}^\dagger\tilde{a}$ and $\tilde{b}^\dagger\tilde{b}$, respectively.

One immediately notices that the terms $\tilde{a}^2$ and $\tilde{b}^2$ in Hamiltonian (7), which resemble the parametric conversions in quantum optics [26,27], serve as the basis for the geometric squeezing. The squeezing parameter $\zeta$ is proportional to the trap anisotropy parameter $\varepsilon$. At the critical rotation velocity $\Omega = \omega$, the three key parameters characterizing $\tilde{h}_0$—$\tilde{\omega}_+ \approx 2\omega$, $\zeta = \varepsilon\omega/2$, and $\tilde{\omega}_- \approx \varepsilon^2\omega/8$—are of zeroth, first, and second order in $\varepsilon$, respectively. For a small $\varepsilon$, $\tilde{\omega}_-$ becomes negligible such that the first two terms of $\tilde{h}_0$ yield the Landau levels: For a given $n_{\tilde{a}}$, different $n_{\tilde{b}}$ provide massive degeneracy; in contrast, states in adjacent $n_{\tilde{a}}$ exhibit an energy gap $\tilde{\omega}_+$. Particularly, states $|n_{\tilde{a}} = 0, n_{\tilde{b}}\rangle$ are called the lowest Landau levels (LLLs).

*Guiding-center mode squeezing.* Consider the following protocol: (1) Prepare the BEC in the ground state of the system with the isotropic irrotational trap (i.e., $\varepsilon = 0$ and $\Omega = 0$). (2) Ramp up the rotation frequency $\Omega$, in which the BEC remains in the isotropic steady state [30]. (3) At $t = 0$, when the critical condition $\Omega = \omega$ is reached, the trap anisotropy $\varepsilon$ is suddenly turned on and the system starts to evolve under Hamiltonian (7). Note that the initial nonrotating state is the same as $|n_{\tilde{a}} = 0, n_{\tilde{b}} = 0\rangle$ up to a correction of $O(\varepsilon^2)$. In the ensuing time evolution, the cyclotron mode is dominated by the first term $\tilde{\omega}_+\tilde{a}^\dagger\tilde{a}$, which thus, to a good approximation, remains in the initial state $|n_{\tilde{a}} = 0\rangle$. In contrast, the time-evolution operator for the guiding-center mode takes the form of the squeezing operator $U_{\tilde{b}}(t) = \exp(-i\zeta t\tilde{b}^2/2 - \text{H.c.})$ with squeezing angle $-\pi/4$, which transforms the BEC into a single-mode squeezed state, i.e., $U_{\tilde{b}}(t)|0, 0\rangle = |0, S(t)\rangle$. During the squeezing, quantum fluctuations behave as

$$\Delta\tilde{X}_{-\pi/4} = \Delta_{\text{SQL}}e^{-\zeta t}, \quad \Delta\tilde{Y}_{\pi/4} = \Delta_{\text{SQL}}e^{\zeta t}, \tag{8}$$

where $\Delta\tilde{X}_{-\pi/4}$ and $\Delta\tilde{Y}_{\pi/4}$ denote the quadrature fluctuations in the $\tilde{X}$-$\tilde{Y}$ phase space, respectively, along the squeezing and antisqueezing directions, and $\Delta_{\text{SQL}} = l_B/\sqrt{2}$ is the standard quantum limit (SQL). In the coordinate $x$-$y$ space, the BEC's density distribution can be obtained as [11,31]

$$\rho(\mathbf{r}, t) \approx |\langle\mathbf{r}|0, S(t)\rangle|^2 = \frac{e^{-[1-\tanh(\zeta t)]\frac{(x+y)^2}{4l_B^2} - [1+\tanh(\zeta t)]\frac{(x-y)^2}{4l_B^2}}}{2\pi l_B^2\cosh(\zeta t)}, \tag{9}$$

which is a 2D Gaussian independently along directions $(x \pm y)/\sqrt{2}$ and of widths $\sqrt{(1+e^{\pm 2\zeta t})/2}l_B$, respectively. In the asymptotic limit $t \to \infty$, the width along the $-\pi/4$ direction converges to $\sigma_{\text{LLL}} = l_B/\sqrt{2}$, while that along the $\pi/4$ direction diverges.

We confirm these results by numerically solving the time-dependent Schrödinger equation based on Eqs. (1) and (2), with the outcome displayed in Fig. 1. Specifically, quadrature fluctuations in the $\tilde{\xi}$-$\tilde{\eta}$ and $\tilde{X}$-$\tilde{Y}$ phase spaces are presented in Figs. 1(a1) and 1(a2), respectively; the density profiles at selected moments are displayed in Figs. 1(b1)–1(b3).

*Floquet protocol.* Now we introduce our Floquet protocol to squeeze the cyclotron mode. The full protocol is similar to what is described above except that the trap anisotropy is periodically modulated as

$$\varepsilon(t) = \varepsilon - 2\varepsilon'\cos(\nu t), \tag{10}$$

where $\varepsilon$ and $\varepsilon'$ are respectively the amplitude of the dc and ac components, and $\nu$ denotes the modulation frequency. The factor 2 is introduced for convenience. Under the same

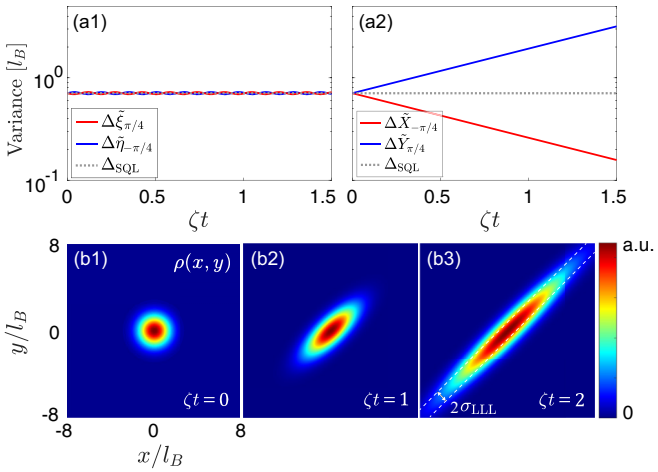


FIG. 1. Guiding-center mode squeezing. (a1) and (a2) show the quadrature fluctuations in the $\tilde{\xi}$-$\tilde{\eta}$ and $\tilde{X}$-$\tilde{Y}$ phase spaces, respectively. (b1)–(b3) display the real-space density distribution $\rho(\mathbf{r},t)$ [in arbitrary units (a.u.)] at selected moments, with white dashed lines indicating $\pm\sigma_{\rm LLL}=\pm l_B/\sqrt{2}$. In our calculation, we take $\varepsilon=0.2$.

transformation $G$, the Hamiltonian now reads [31]

$$\begin{aligned}\tilde{h}_0(t)=&\,\tilde{\omega}_+\tilde{a}^\dagger\tilde{a}+\tilde{\omega}_-\tilde{b}^\dagger\tilde{b}-h_{\rm ab}(t)\\&-\left\{\left[\frac{\zeta}{2}+\zeta'\cos(\nu t)\right]\tilde{a}^2\right.\\&\left.-\left[\frac{\zeta}{2}-\zeta'\cos(\nu t)\right]\tilde{b}^2+\text{H.c.}\right\}.\end{aligned}\tag{11}$$

Comparing with Eq. (7), the ac driving provides an alternating squeezing parameter with $\zeta'=\varepsilon'\omega/2s$, and $h_{\rm ab}(t)=2\zeta'\cos(\nu t)(\tilde{a}^\dagger\tilde{b}+\tilde{b}^\dagger\tilde{a})$ denoting the coupling between the two modes.

Taking another unitary transformation $W(t)=e^{i\tilde{\omega}_+t\tilde{a}^\dagger\tilde{a}}$, the Hamiltonian is expressed as

$$\begin{aligned}\tilde{h}_0^W(t)=&\,\tilde{\omega}_-\tilde{b}^\dagger\tilde{b}-[2\zeta'e^{i\tilde{\omega}_+t}\cos(\nu t)\tilde{a}^\dagger\tilde{b}+\text{H.c.}]\\&-\left\{\left[\frac{\zeta}{2}+\zeta'\cos(\nu t)\right]e^{2i\tilde{\omega}_+t}\tilde{a}^2\right.\\&\left.-\left[\frac{\zeta}{2}-\zeta'\cos(\nu t)\right]\tilde{b}^2+\text{H.c.}\right\}.\end{aligned}\tag{12}$$

Now, the term $\tilde{a}^2$, as well as the coupling $\tilde{a}^\dagger\tilde{b}$, depends on both $\tilde{\omega}_+$ and $\nu$. We find that, when the modulation frequency is set to $\nu=2\tilde{\omega}_+=2(s\omega+\Omega)$, the Floquet effective Hamiltonian takes the form of

$$\tilde{h}_0^{\rm eff}\equiv\frac{1}{T}\int_0^T\tilde{h}_0^W(t)\,dt=\tilde{\omega}_-\tilde{b}^\dagger\tilde{b}-\left(\frac{\zeta'}{2}\tilde{a}^2-\frac{\zeta}{2}\tilde{b}^2+\text{H.c.}\right),\tag{13}$$

where $T\equiv 2\pi/\tilde{\omega}_+=4\pi/\nu$ is the stroboscopic period. The time integral in Eq. (13) kept all the zero-frequency terms in $\tilde{h}_0^W$ but erased all nonzero-frequency terms.

Equation (13) is a key result of this Letter: Compared to Eq. (7), the term $\tilde{\omega}_+\tilde{a}^\dagger\tilde{a}$ is absent in the effective Hamiltonian $\tilde{h}_0^{\rm eff}$, i.e., the Landau-level gap that previously prevented squeezing in the cyclotron mode is now eliminated by the Floquet driving. As a consequence, the term $\sim\tilde{a}^2+(\tilde{a}^\dagger)^2$ now can dominate the dynamics and generate squeezing in the cyclotron mode. Furthermore, at the critical rotation with $\Omega=\omega$ and hence $\tilde{\omega}_-\approx 0$, $\tilde{h}_0^{\rm eff}$ still allows squeezing of the guiding-center mode. As a consequence, both modes can be squeezed simultaneously, resulting in two-mode geometric squeezing. Below, we will discuss these two cases in detail.

*Cyclotron-mode squeezing.* By turning off the dc component, i.e., setting $\varepsilon=0$, the $\tilde{b}^2$ term in $\tilde{h}_0^{\rm eff}$ vanishes and the guiding-center mode is not squeezed. In the critical case $\Omega=\omega$, we simply have $s=1$, $\nu=4\omega$, and $\zeta'=\varepsilon'\omega/2$. The stroboscopic dynamics at moments $t=nT$ ($n$ being a non-negative integer) is governed by the Floquet evolution operator $U_{\tilde{a}}^n=\exp(i\zeta' nT\tilde{a}^2/2-\text{H.c.})$, which is also a squeezing operator and drives the cyclotron mode into a squeezed state, i.e., $U_{\tilde{a}}^n|0,0\rangle=|S,0\rangle$. The properties of $|S,0\rangle$ are quite similar to the guiding-center squeezed state $|0,S\rangle$ discussed previously, except that the squeezing now exists in the $\tilde{\xi}$-$\tilde{\eta}$ phase space. The corresponding quadrature fluctuations behave as

$$\Delta\tilde{\xi}_{\pi/4}=\Delta_{\rm SQL}e^{-\zeta' nT},\quad \Delta\tilde{\eta}_{-\pi/4}=\Delta_{\rm SQL}e^{\zeta' nT}.\tag{14}$$

The real-space density distribution can be worked as [31]

$$\rho(\mathbf{r},t=nT)=\frac{e^{-[1-\tanh(\zeta' t)]\frac{(x+y)^2}{4l_B^2}-[1+\tanh(\zeta' t)]\frac{(x-y)^2}{4l_B^2}}}{2\pi l_B^2\cosh(\zeta' t)}.\tag{15}$$

which is also a 2D Gaussian with minimal width along the $-\pi/4$ direction and converging to $\sigma_{\rm LLL}=l_B/\sqrt{2}$ as $n\to\infty$.

The complete dynamics can be obtained by numerically solving the time-dependent Schrödinger equation, with results presented in Fig. 2(a), where Figs. 2(a1) and 2(a2) show the fluctuations in the $\tilde{\xi}$-$\tilde{\eta}$ and $\tilde{X}$-$\tilde{Y}$ phase spaces, and Figs. 2(a3)–2(a8) illustrate $\rho(\mathbf{r},t)$ at selected moments. It is shown that the quadrature variance of the $\tilde{a}$ mode has been considerably squeezed, whereas that in the $\tilde{b}$ mode remains unsqueezed, as anticipated. At stroboscopic moments $t=nT$ (indicated by thick vertical lines), $\Delta\tilde{\xi}_{\pi/4}$ and $\Delta\tilde{\eta}_{-\pi/4}$ respectively exhibit exponential squeezing and antisqueezing, confirming the analytical results in Eq. (14).

Within a stroboscopic period $T$, quantum fluctuations oscillate, accompanied by the clockwise rotation of the density profile, which can be understood as follows. For any initial time $t_0$, the Floquet Hamiltonian $\tilde{h}_0^{t_0}$ characterizes the physics at moments $t=t_0+nT$, and the effective Hamiltonian $\tilde{h}_0^{\rm eff}$ shown in Eq. (13) represents the specific case for $t_0=0$. It is straightforward to show that [31]

$$\tilde{h}_0^{t_0}=\tilde{\omega}_-\tilde{b}^\dagger\tilde{b}-\left[\frac{\zeta'}{2}(e^{-i\varphi/2}\tilde{a})^2-\frac{\zeta}{2}\tilde{b}^2+\text{H.c.}\right],\tag{16}$$

implying that the squeezing angle in the $\tilde{\xi}$-$\tilde{\eta}$ phase space is altered by $\varphi/2=-\nu t_0/2$. Particularly for $t_0$ being odd multiples of $T/4$, $\varphi=\pm\pi\ [\text{mod}\,2\pi]$ (equivalently $\zeta'\to-\zeta'$ for $\tilde{h}_0^{\rm eff}$), which leads to a swap between squeezing and antisqueezing directions compared to the case of $t_0=\varphi=0$. This also explains the alternating long and short axis of the density distribution $\rho(\mathbf{r})$ [see Eq. (15) and Fig. 2(a6)].

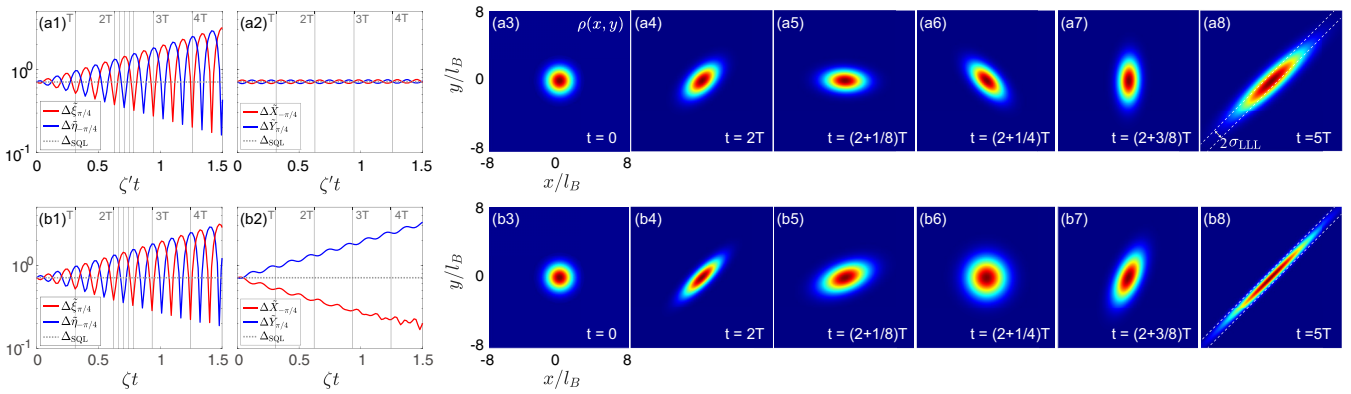


FIG. 2. Floquet geometric squeezing. The upper row (a) illustrates the cyclotron-mode squeezing with $\varepsilon = 0$ and $\varepsilon' = 0.2$; the lower row (b) shows the two-mode squeezing with $\varepsilon = \varepsilon' = 0.2$. In each row, the first two panels show the quadrature fluctuations in the $\tilde{\xi}$-$\tilde{\eta}$ and $\tilde{X}$-$\tilde{Y}$ phase spaces; vertical lines mark the stroboscopic moments $t = nT$, with $T = 2\tilde{\omega}_+ \approx 4\omega$; the remaining six panels display the density distribution $\rho(\mathbf{r}, t)$ at selected moments. In the Supplemental Material (SM) [31], we provide animations of $\rho(\mathbf{r}, t)$ for various types of geometric squeezing.

*Two-mode squeezing.* We are now ready to discuss the two-mode squeezing protocol where $\varepsilon(t)$ includes both the dc and ac components. Here, we specifically examine the case of $\zeta' = \zeta$, which can be satisfied by setting $\varepsilon' = \varepsilon$ and $\Omega = (1/2 + \sqrt{1+\varepsilon^2}/2)^{1/2}\omega \approx (1 + \varepsilon^2/8)\omega$. A more general discussion for $\zeta' \neq \zeta$ can be found in the SM [31]. In the current situation, the stroboscopic evolution $U^n = \exp[i\zeta nT(\tilde{a}^2/2 - \tilde{b}^2/2) - \text{H.c.}]$ at moments $t = nT$ is a squeezing operator for both the $\tilde{a}$ and $\tilde{b}$ modes, leading to the two-mode squeezed state $U^n|0,0\rangle = |S,S\rangle$.

The stroboscopic dynamics manifests that quantum fluctuations in both phase spaces scale exponentially, following Eqs. (8) and (14), as numerically confirmed by Figs. 2(b1) and 2(b2). The density distribution of $|S,S\rangle$ is given by [31]

$$\rho(\mathbf{r}, t = nT) = \frac{1}{2\pi l_B^2} \exp\left[-\frac{(x+y)^2}{4l_B^2 e^{2\zeta t}} - \frac{(x-y)^2}{4l_B^2 e^{-2\zeta t}}\right], \quad (17)$$

with minimal width along the $-\pi/4$ direction being $e^{-\zeta nT} l_B$. Notably, in contrast to the single-mode squeezing cases presented in Eqs. (9) and (15) where the minimal width asymptotically saturates to $\sigma_{\rm LLL}$, here the minimal width exponentially decreases as $n$ increases and can fall below $\sigma_{\rm LLL}$. Note that although Eq. (17) indicates that the minimal width tends to zero for large $n$, this result is obtained under the effective Floquet Hamiltonian $\tilde{h}_0^{\rm eff}$ where high-order corrections are neglected. A calculation based on high-frequency expansion shows that the next-order corrections are $\tilde{a}^\dagger\tilde{a}$ and $\tilde{b}^\dagger\tilde{b}$ with strength $\propto \zeta^2/\tilde{\omega}_+$ [31]. Consequently, the squeezing behaviors will be limited to a timescale $\sim\omega/\zeta^2$ which prevents the width going all the way to zero. Nevertheless, the statement that the minimal width can fall below $\sigma_{\rm LLL}$ is robust as confirmed by our numerical simulation using the original time-dependent Hamiltonian and illustrated in Fig. 2(b8).

Furthermore, the dynamics at quarter periods $t = nT/4$ ($n$ being odd) manifest isotropic density profiles, as shown in Fig. 2(b6). Again, the Floquet Hamiltonian $\tilde{h}_0^{t_0}$ is now equivalent to $\tilde{h}_0^{\rm eff}$ subject to $\zeta' \to -\zeta'$, based on which we can obtain [31]

$$\rho(\mathbf{r}, t = nT/4) = \frac{1}{2\pi l_B^2 \cosh(2\zeta t)} \exp\left[-\frac{x^2+y^2}{2l_B^2\cosh(2\zeta t)}\right], \quad (18)$$

which is a 2D isotropic Gaussian, with width $\sqrt{\cosh(2\zeta t)} l_B$ monotonically increasing in $t$ and scaling exponentially $e^{\zeta t} l_B$ for $t \gg 1/2\zeta$.

We additionally remark that, although our discussion above has assumed a small anisotropy ($\varepsilon \ll 1$), numerical calculation [31] shows that the results remain valid for a sizable anisotropy.

*Interacting BECs.* So far we have ignored interatomic interactions. The case would become more complicated when atomic collisions are included, with the system now being described by the Gross-Pitaevskii equation (GPE)

$$i\dot{\psi} = (h_0 + g|\psi|^2)\psi, \quad (19)$$

where $\psi(\mathbf{r}, t)$ is the mean-field wave function, and $g = \sqrt{8\pi\omega_z/m}a_s$ denotes the two-body interaction strength in two dimension, with $a_s$ the $s$-wave scattering length and $\omega_z$ the longitudinal trapping frequency.

For sufficiently small $g$, the single-particle physics presented above remains qualitatively unchanged. However, when the BEC operates within the Thomas-Fermi (TF) regime, i.e., the interaction energy significantly exceeds the kinetic energy, the $g$ term begins to markedly influence the squeezing dynamics. To illustrate the TF case, we implement our protocol by numerically propagating the GPE, with the results for the cyclotron-mode and the two-mode squeezing being respectively shown in Figs. 3(a) and 3(b). The parameters used are close to those in the experiment [11], i.e., considering $N = 5 \times 10^4$ Na atoms with $a_s \approx 63a_0$ ($a_0$ being the Bohr radius); the trapping frequencies are $\omega = 88.6 \times (2\pi)$ Hz and $\omega_z = \sqrt{8}\omega$. In this case, the BEC enters the deep Thomas-Fermi regime, with the wave-packet width being much larger than the harmonic oscillator length (see the animations in Supplemental Material [31]). The initial state is the irrotational ground state of the interacting BEC at $\Omega = 0$

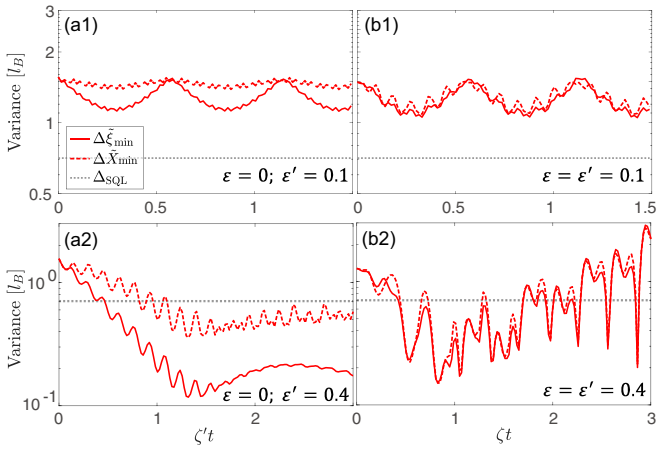


FIG. 3. Dynamics of $\Delta\tilde{\xi}_{\min}$ (solid lines) and $\Delta\tilde{X}_{\min}$ (dashed lines) for interacting BECs. (a1) and (b1) correspond to the cases of the cyclotron-mode and the two-mode squeezings, respectively, with $(\varepsilon, \varepsilon') \sim 0.1$. (a2) and (b2) present the results for $(\varepsilon, \varepsilon') \sim 0.4$. See the SM [31] for animations of $\rho(\mathbf{r}, t)$.

and $\varepsilon(t) = 0$, which remains stable as $\Omega$ is linearly ramped up to the critical value $\omega$ [14,30]. Then, the system begins to evolve under $\varepsilon(t) \neq 0$.

For the interacting BEC, the squeezing/antisqueezing direction may not be exactly along $\pm\pi/4$. Hence, we characterize the squeezing by $\Delta\tilde{\xi}_{\min}$ and $\Delta\tilde{X}_{\min}$, respectively denoting the minimum quantum fluctuations in the $\tilde{\xi}$-$\tilde{\eta}$ and $\tilde{X}$-$\tilde{Y}$ phase spaces. Figures 3(a1) and 3(b1) present the minimum fluctuations for the cases of small anisotropy $(\varepsilon, \varepsilon') \sim 0.1$. The results indicate that neither the single cyclotron mode nor the two-mode state can be squeezed effectively, manifested by the periodic oscillations of $\Delta\tilde{\xi}_{\min}$ and $\Delta\tilde{X}_{\min}$. The oscillation period $T \approx 0.56\omega^{-1}$ is insensitive to $g$ when the BEC enters the TF regime. These phenomena imply that the interacting BEC is in a near-equilibrium state, exhibiting certain collective oscillations.

We further find that increasing the anisotropy helps disrupt the periodicity and yields considerable squeezing. Figures 2(a2) and 2(b2) display the squeezing dynamics for $(\varepsilon, \varepsilon') \sim 0.4$, with all other parameters remaining unchanged. Both scenarios can yield squeezings $\geqslant -10\log_{10}(0.15/\Delta_{\rm SQL}) \gtrsim 6.7$ dB. In real space, $\rho(\mathbf{r}, t)$ exhibits behaviors qualitatively similar to those of the noninteracting cases shown in Fig. 2: For $\tilde{a}$-mode squeezing, $\rho(\mathbf{r}, t)$ is elongated during the rotation process, whereas for two-mode squeezing, $\rho(\mathbf{r}, t)$ alternates between isotropic and anisotropic, accompanied by an increase in amplitude.

*Conclusion*. We have introduced a Floquet protocol by periodically modulating the anisotropy of the trapping potential, resulting in squeezing of both the guiding-center and the cyclotron modes in a rotating BEC. Such two-mode squeezing exhibits a richer set of dynamics in comparison to the one-mode squeezing previously shown and can achieve a wave-packet width below the lowest Landau level limit. We also demonstrated the protocol's effectiveness in interacting BECs for relatively large anisotropy. Our work provides a versatile tool for realizing diverse geometrically squeezed states in rotating quantum gases, offering prospects for experimental realization within current experimental capabilities.

*Acknowledgments.* We would like to thank Jing Zhang for the valuable discussion. L.C. acknowledges support from the NSF of China (Grant No. 12174236) and from the fund for the Shanxi 1331 Project; Y.Z. acknowledges support from the NSF of China (Grant No. 12474492). H.P. acknowledges support from the U.S. NSF (Grant No. PHY-2207283) and the Welch Foundation (Grant No. C-1669).

[1] N. Goldman, J. C. Budich, and P. Zoller, Topological quantum matter with ultracold gases in optical lattices, Nat. Phys. **12**, 639 (2016).
[2] T. Ozawa and H. M. Price, Topological quantum matter in synthetic dimensions, Nat. Rev. Phys. **1**, 349 (2019).
[3] N. R. Cooper, J. Dalibard, and I. B. Spielman, Topological bands for ultracold atoms, Rev. Mod. Phys. **91**, 015005 (2019).
[4] S. Viefers, Quantum Hall physics in rotating Bose–Einstein condensates, J. Phys.: Condens. Matter **20**, 123202 (2008).
[5] N. R. Cooper, Rapidly rotating atomic gases, Adv. Phys. **57**, 539 (2008).
[6] A. L. Fetter, Rotating trapped Bose-Einstein condensates, Rev. Mod. Phys. **81**, 647 (2009).
[7] K. W. Madison, F. Chevy, W. Wohlleben, and J. Dalibard, Vortex formation in a stirred Bose-Einstein condensate, Phys. Rev. Lett. **84**, 806 (2000).
[8] J. R. Abo-Shaeer, C. Raman, J. M. Vogels, and W. Ketterle, Observation of vortex lattices in Bose-Einstein condensates, Science **292**, 476 (2001).
[9] V. Schweikhard, I. Coddington, P. Engels, V. P. Mogendorff, and E. A. Cornell, Rapidly rotating Bose-Einstein condensates in and near the lowest Landau level, Phys. Rev. Lett. **92**, 040404 (2004).
[10] V. Bretin, S. Stock, Y. Seurin, and J. Dalibard, Fast rotation of a Bose-Einstein condensate, Phys. Rev. Lett. **92**, 050403 (2004).
[11] R. J. Fletcher, A. Shaffer, C. C. Wilson, P. B. Patel, Z. Yan, V. Crépel, B. Mukherjee, and M. W. Zwierlein, Geometric squeezing into the lowest Landau level, Science **372**, 1318 (2021).
[12] B. Mukherjee, A. Shaffer, P. B. Patel, Z. Yan, C. C. Wilson, V. Crépel, R. J. Fletcher, and M. Zwierlein, Crystallization of bosonic quantum Hall states in a rotating quantum gas, Nature (London) **601**, 58 (2022).
[13] T.-L. Ho, Bose-Einstein condensates with large number of vortices, Phys. Rev. Lett. **87**, 060403 (2001).
[14] A. Recati, F. Zambelli, and S. Stringari, Overcritical rotation of a trapped Bose-Einstein condensate, Phys. Rev. Lett. **86**, 377 (2001).
[15] N. Regnault and T. Jolicoeur, Quantum Hall fractions in rotating Bose-Einstein condensates, Phys. Rev. Lett. **91**, 030402 (2003).

[16] E. B. Sonin, Ground state and Tkachenko modes of a rapidly rotating Bose-Einstein condensate in the lowest-Landau-level state, Phys. Rev. A **72**, 021606(R) (2005).

[17] S. Sinha and G. V. Shlyapnikov, Two-dimensional Bose-Einstein condensate under extreme rotation, Phys. Rev. Lett. **94**, 150401 (2005).

[18] A. L. Fetter, Lowest-Landau-level description of a Bose-Einstein condensate in a rapidly rotating anisotropic trap, Phys. Rev. A **75**, 013620 (2007).

[19] S. Furukawa and M. Ueda, Quantum Hall states in rapidly rotating two-component Bose gases, Phys. Rev. A **86**, 031604(R) (2012).

[20] N. Regnault and T. Senthil, Microscopic model for the boson integer quantum Hall effect, Phys. Rev. B **88**, 161106(R) (2013).

[21] D. Tong, Lectures on the quantum Hall effect, arXiv:1606.06687.

[22] D. Yoshioka, *The Quantum Hall Effect* (Springer, Berlin, 2002).

[23] V. Sharma and E. J. Mueller, Rotating Bose gas dynamically entering the lowest Landau level, Phys. Rev. A **105**, 023310 (2022).

[24] V. Crépel, R. Yao, B. Mukherjee, R. Fletcher, and M. Zwierlein, Geometric squeezing of rotating quantum gases into the lowest Landau level, C. R. Phys. **24**, 241 (2024).

[25] A. Shaffer, Bosonic quantum Hall states from rapidly rotating Bose-Einstein condensates, Dissertation, Massachusetts Institute of Technology, 2023.

[26] L.-A. Wu, H. J. Kimble, J. L. Hall, and H. Wu, Generation of squeezed states by parametric down conversion, Phys. Rev. Lett. **57**, 2520 (1986).

[27] L.-A. Wu, M. Xiao, and H. J. Kimble, Squeezed states of light from an optical parametric oscillator, J. Opt. Soc. Am. B **4**, 1465 (1987).

[28] M. O. Scully and M. S. Zubairy, *Quantum Optics* (Cambridge University Press, Cambridge, UK, 1997).

[29] D. F. Walls and G. J. Milburn, *Quantum Optics*, 2nd ed (Springer, Berlin, 2008).

[30] For the isotropic system with sufficiently large $\Omega$, the nonrotating isotropic state is no longer the ground state of the system. However, it remains a dynamically stable state for both the noninteracting BEC and interacting BECs with $g > 0$ [14]. The ramping time of $\Omega$ should be much smaller than the BEC's coherence time.

[31] See Supplemental Material at http://link.aps.org/supplemental/10.1103/PhysRevA.111.L011303 for more calculation details and the animations of $\rho(\mathbf{r}, t)$ to illustrate various types of squeezing dynamics. Specifically, animations (1)–(3) correspond to the guiding-center mode, cyclotron-mode, and two-mode squeezings for noninteracting BECs. Animations (4) and (5) show the cyclotron-mode, and two-mode squeezings for interacting BECs under $(\varepsilon, \varepsilon') \sim 0.1$. Animations (6) and (7) show the cyclotron-mode, and two-mode squeezings for interacting BECs under $(\varepsilon, \varepsilon') \sim 0.4$, which includes Refs. [21,32,33].

[32] A. Eckardt and E. Anisimovas, High-frequency approximation for periodically driven quantum systems from a Floquet-space perspective, New J. Phys. **17**, 093039 (2015).

[33] R. A. Fisher, M. M. Nieto, and V. D. Sandberg, Impossibility of naively generalizing squeezed coherent states, Phys. Rev. D **29**, 1107 (1984).